Applications of Artificial Neural Networks to RF and Microwave Measurements

Jeffrey A. Jargon,[1] K. C. Gupta,[2] Donald C. DeGroot[1]

[1]National Institute of Standards and Technology, RF Electronics Group, 325 Broadway, Boulder, Colorado 80303
[2]Center for Advanced Manufacturing and Packaging of Microwave, Optical, and Digital Electronics (CAMPmode), University of Colorado at Boulder, Boulder, Colorado 80309

Received 21 April 2001; revised 24 July 2001

ABSTRACT: This article describes how artificial neural networks (ANNs) can be used to benefit a number of RF and microwave measurement areas including vector network analysis (VNA). We apply ANNs to model a variety of on-wafer and coaxial VNA calibrations, including open-short-load-thru (OSLT) and line-reflect-match (LRM), and assess the accuracy of the calibrations using these ANN-modeled standards. We find that the ANN models compare favorably to benchmark calibrations throughout the frequencies they were trained for. We summarize other current applications of ANNs, including the determination of permittivities of liquids from the reflection coefficient measurements of an open-ended coaxial probe and the determination of moisture content of wheat from free-space transmission coefficient measurements. We also discuss some potential applications of ANN models related to power measurements, material characterization, and the comparison of nonlinear vector network analyzers. © 2002 John Wiley & Sons, Inc. Int J RF and Microwave CAE 12: 3–24, 2002.

Keywords: application; artificial neural network; calibration, measurement; microwave, model; network analyzer; standards

1. INTRODUCTION

Artificial neural networks (ANNs) are neuroscience-inspired computational tools that are trained using input-output data to generate a desired mapping from an input stimulus to the targeted output. ANNs consist of multiple layers of processing elements called neurons. Each neuron is linked to other neurons in neighboring layers by varying coefficients that represent the strengths of these connections. Learning is accomplished by adjusting these coefficients until the network provides output results that meet prescribed values.

ANNs have been applied to such diverse areas as speech and pattern recognition, financial and economic forecasting, telecommunications, and nuclear power plant diagnosis, and have recently been introduced into the area of microwave engineering [1]. In particular, researchers have successfully used ANNs to model microstrip vias [2], packaging and interconnects [3], spiral inductors [4], MESFET devices [5], CPW circuit components [6], effective dielectric constant of microstrip lines [7], and HBT amplifiers [8], to name just a few.

In addition to modeling devices and circuits using simulated data, ANNs also have many potential applications in the area of RF and microwave measurements, which is the subject of this article. Here, we describe how ANNs can be used to benefit a variety of measurement areas

Correspondence to: Jeffrey A. Jargon; e-mail: jargon@boulder.nist.gov.

DOI 10.1002/mmce.10014

including power, material characterization, and most notably vector network analysis.

Vector network analyzers (VNAs) are one of the most versatile instruments in the RF and microwave industry. They can be found in calibration facilities, research laboratories, design facilities, and on production lines. VNAs are used to measure complex scattering parameters of devices and circuits. Engineers use them to verify their designs, confirm proper performance, and diagnose failures. The accuracy of a VNA measurement is highly dependent on its calibration, which accounts for imperfections in the instrument such as impedance mismatch, loss in the cables and connectors, the frequency response of the source and receiver, and directivity, and cross talk due to signal leakage. There are a wide variety of calibration methods available to VNA users, most of which can be classified into one of two categories depending on the type of calibration standards used.

The first category makes use of transmission lines as standards, and includes such calibration methods as thru-reflect-line (TRL) [9] and multiline TRL [10]. Multiline TRL is the most accurate means of VNA calibration and is especially useful for on-wafer environments, because the characteristic impedance can be calculated from dimensional measurements of the standards, which simply consist of a number of transmission lines of varying line lengths and a reflective termination. In an on-wafer environment, the disadvantages of this method are that it requires a lot of real estate on the wafer, due to the numerous long lines required for an accurate calibration, and the different lengths of line necessitate changing the separation between probes during the calibration process. In a coaxial environment, the disadvantages are that a large number of expensive airline standards and numerous interconnects are required.

Consequently, a second category of VNA calibrations, which makes use of compact and lumped-element standards, is often preferred. The most common of these calibrations are the open-short-load-thru (OSLT) and the line-reflect-match (LRM) [11] methods. The trade-off is that these methods tend to be less accurate, because it is more difficult to calculate the reflection coefficients of the standards from independent physical measurements. But, if the compact calibration kits are characterized using a benchmark calibration, such as multiline TRL, then it is possible to perform an accurate lumped-element calibration.

Once the lumped-element standards for a given calibration kit are characterized, we must decide whether to develop a model for each of the standards or to directly use the measurement data obtained from the benchmark calibration. Recently, we have applied ANNs to improve the modeling of lumped-element standards in both on-wafer and coaxial environments [12–15]. We have shown that ANN models offer a number of advantages over the use of calibrated-measurement data files and equivalent circuit models, namely, the following: (1) they do not require detailed physical models; (2) calibration times can be reduced because only a few training points are required to accurately model the standards; (3) ANN model descriptions are much more compact than large measurement files; (4) ANN models, trained on only a few measurement points, can be much more accurate than direct calibrations when limited data are available; and (5) they are less susceptible to the noise inherent in measured data.

In this article, we summarize our work in this area, describing how we have successfully modeled on-wafer OSLT standards, in one case assuming that the standards can be reproduced from wafer to wafer with little variation, and in another case where the loads exhibit significant difference among the wafers studied. We also describe how we modeled load standards to improve both on-wafer and coaxial LRM calibrations.

In addition to describing how ANNs can be used to improve VNA calibrations, we summarize other current applications of ANNs to RF and microwave measurements. In particular, we discuss how two groups of researchers have used ANNs to model the transformation from measured reflection coefficients to permittivity values for liquids. We also examine how scientists have used ANNs to determine the moisture content of wheat from measurements of microwave transmission coefficients.

We also discuss some potential applications of ANNs to RF and microwave power measurements, material characterization, and comparisons of nonlinear vector network analyzers. Specifically, we show how ANN models may be used to determine the complex permittivity of low-loss dielectric materials from measured shifts in resonant frequency and quality factor using a split-post resonator. We illustrate how lengthy measurement times for microcalorimeter measurements can possibly be reduced without noticeably degrading accuracy. Finally, we explore the possibility

of using ANN models to compare nonlinear vector network analyzers, where directly comparing measured parameters is not possible in assessing instrument accuracy.

2. ARTIFICIAL NEURAL NETWORKS

One popular type of ANN architecture, that was used in our work, is a feed-forward, three-layer perceptron structure (MLP3) consisting of an input layer, a hidden layer, and an output layer, as shown in Figure 1. The hidden layer allows complex models of input–output relationships.

ANNs learn relationships among sets of input–output data that are characteristic of the device or system under consideration. After the input vectors are presented to the input neurons and output vectors are computed, the ANN outputs are compared to the desired outputs and errors are calculated. Error derivatives are then calculated and summed for each weight, until all of the training sets have been presented to the network. The error derivatives are used to update the weights for the neurons, and training continues until the errors become no greater than prescribed values. In Sections 3–6, we have utilized software developed by Zhang et al. [16] to construct our ANN models.

3. ON-WAFER OSLT

The OSLT calibration [11] is one of the most widely used techniques for calibrating VNAs. It is mainly used with devices that contain coaxial or waveguide interfaces, but it is also applied often to on-wafer environments such as microstrip and coplanar waveguide (CPW). The calibration procedure consists of a "thru" connection of the two VNA ports as well as the measurement (on both ports) of three one-port standards, typically a nominal open, a nominal short, and a nominally-matched load. None of these standards needs to be ideal, but we must know their reflection coefficients. In practice, our definition of these reflection-coefficient values is typically drawn from a model of the standard.

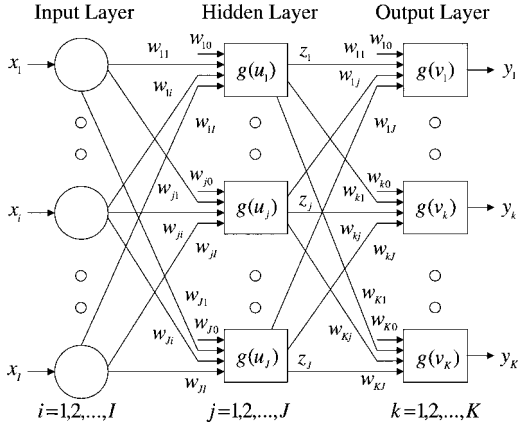

Figure 1. Artificial neural network architecture.

Manufacturers of calibration kits typically provide a description of the standards based on equivalent-circuit parameters, known as Calibration Kit Parameters [17, 18], or Calibration Component Coefficients [19]. These parameters assume single, real values for both load impedance and characteristic impedance and describe the open-and short-circuit terminations as frequency-polynomials of capacitance and inductance, respectively. With coaxial and waveguide standards, the equivalent circuit approximations have worked to the satisfaction of most users, but for on-wafer standards, a recent study [20] reported errors in scattering parameters of up to 0.5. Considering that the maximum possible value for passive devices is a magnitude of 1, such errors are clearly unacceptable. DeGroot et al. [21] recently documented the OSLT models and developed a general description of transmission lines to express offset reflection standards and finite-length thru standards that accounts for lossy environments with complex impedance. However, implementing this more general description still requires physical models or measurement data of each for the individual standards.

Here, we apply ANNs to improve the modeling of on-wafer OSLT standards used for calibrating VNAs [12]. The ANNs are trained with measurement data obtained from a benchmark multiline TRL calibration. We assess the accuracy of an OSLT calibration using these ANN-modeled standards and find that it compares favorably (less than a 0.02 difference in magnitude) to the benchmark multiline TRL calibration over a 40 GHz bandwidth. We also quantify the training errors and training times as a function of both the number of training points and the number of neurons in the hidden layer.

3.1. Modeling the Standards

In this study, the OSLT and multiline TRL standards and devices were constructed of CPW transmission lines fabricated with 1.5 μm thick

gold conductors evaporated on 500 μm thick semi-insulating GaAs [22]; the gold center conductor was 73 μm wide and separated from the ground plane by 49 μm gaps. The five line standards included a 0.55-mm thru line and four additional lines that were 2.135, 3.2, 6.565, and 19.695 mm longer. The load standard was fabricated by terminating a 275-μm section of the CPW with a single 73 μm by 73 μm nickel–chromium thin-film resistor. All the standards were measured using on-wafer probes. The OSLT open circuit was defined by lifting the probe heads-off the wafer, as recommended by probe manufacturers. For each standard, we measured scattering parameters at 192 frequencies from 0.5 to 40 GHz.

Once the OSLT standards had been characterized using a multiline TRL calibration, we determined how many neurons in the hidden layer were required to develop accurate ANN models. Figure 2 illustrates the results for S_{11} of the open, short, and load, and for S_{21} of the thru. Each standard had different errors, but no discernable improvements could be seen for more than five neurons.

After we decided that five hidden neurons were sufficient, we studied how many training points were required to accurately model each standard. We trained each standard using all 192 points, and then tried smaller subsets of the measurement points, namely 3, 5, 9, and 41 points. Figures 3 and 4 show the magnitudes of the vector differences of $S_{11}(|\Delta S_{11}|)$ between the measured data and the ANN models for various numbers of training points for the open and the load standards, respectively. From these two plots, we see that the ANN model of the open standard agrees with measurement data to within 0.015 using as few as five training points. We also see that the ANN model of the load standard agrees with measurement data to within 0.04 for most frequencies using as few as nine training points.

Our observation that only a few training points are sufficient to model our standards highlights an important advantage in using ANN models over calibrated measurement data files. We found that it is possible to cut down on calibration times by measuring only a few frequency points and developing an ANN model rather than measuring numerous points and dealing with large data files. The ANN model, trained on only a few measurement points, can be much more accurate than linearly interpolating, as is commonly done in practice. For example, if one were to measure the load standard at five points and perform linear interpolation between frequencies, as shown in Figure 5, then the maximum error would be 0.045, as opposed to only 0.016 for the ANN model,

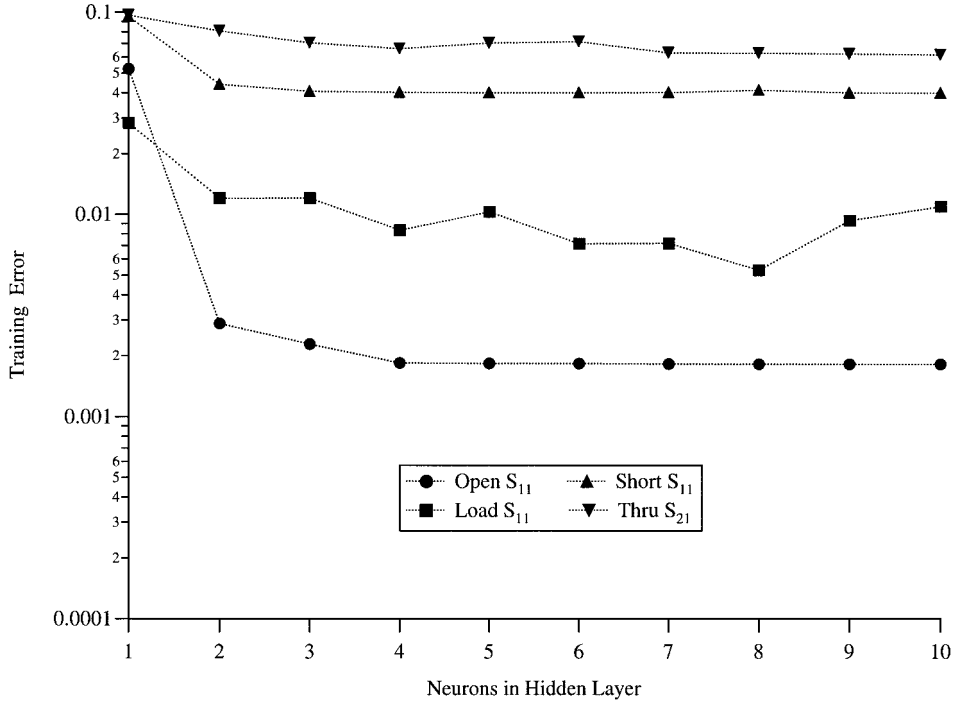

Figure 2. Training error versus the number of neurons in the hidden layer for various OSLT calibration standards.

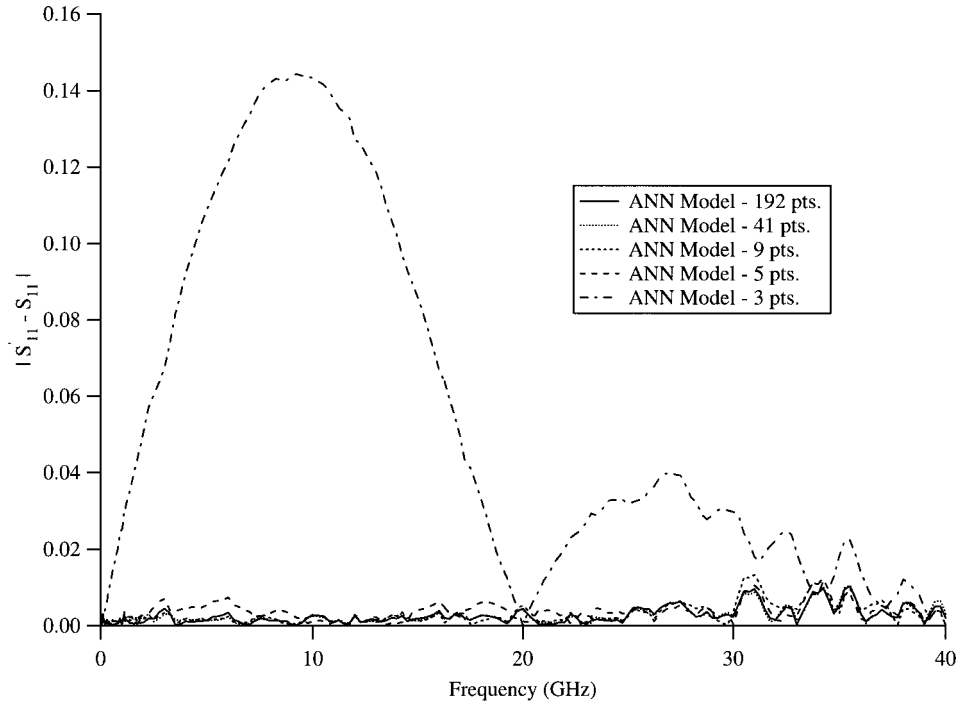

Figure 3. Magnitude of the ANN-modeled reflection coefficient errors ($|\Delta S_{11}|$) for the open standard with varying numbers of training points.

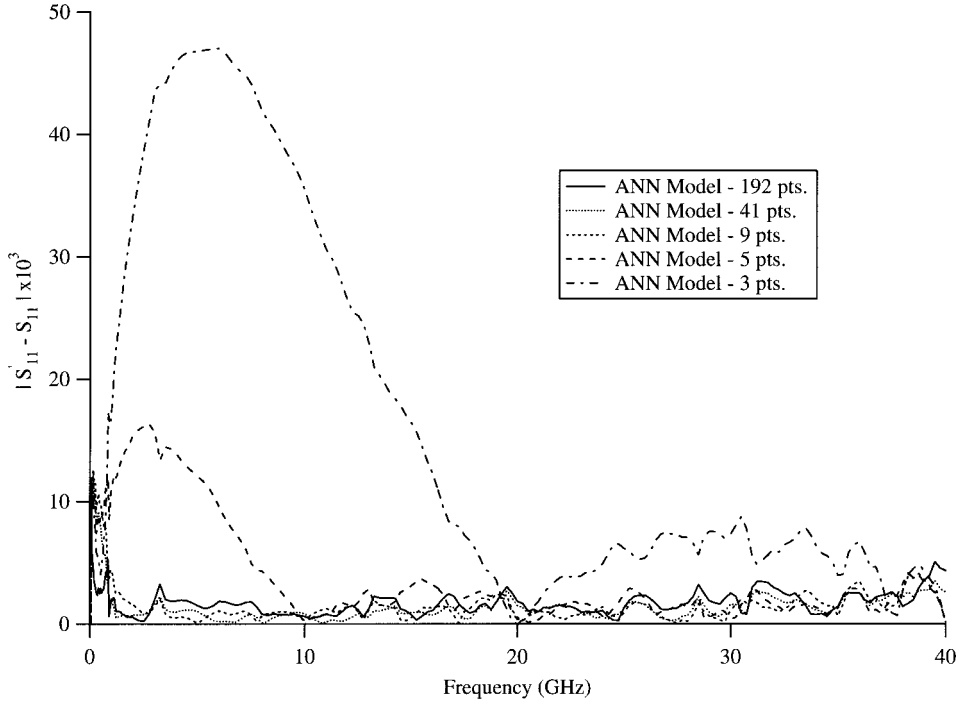

Figure 4. Magnitude of the ANN-modeled reflection coefficient errors ($|\Delta S_{11}|$) for the load standard with varying numbers of training points.

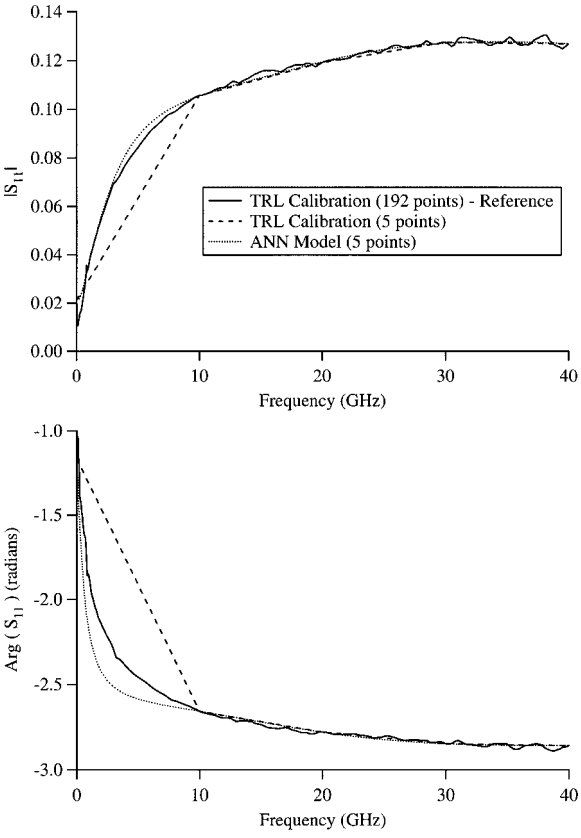

Figure 5. Comparison of magnitude and phase of the reflection coefficients [$|S_{11}|$ and Arg(S_{11})] for the load standard using an ANN model trained with 5 points, linear interpolation with TRL using the same 5 points, and TRL with 192 points as the reference.

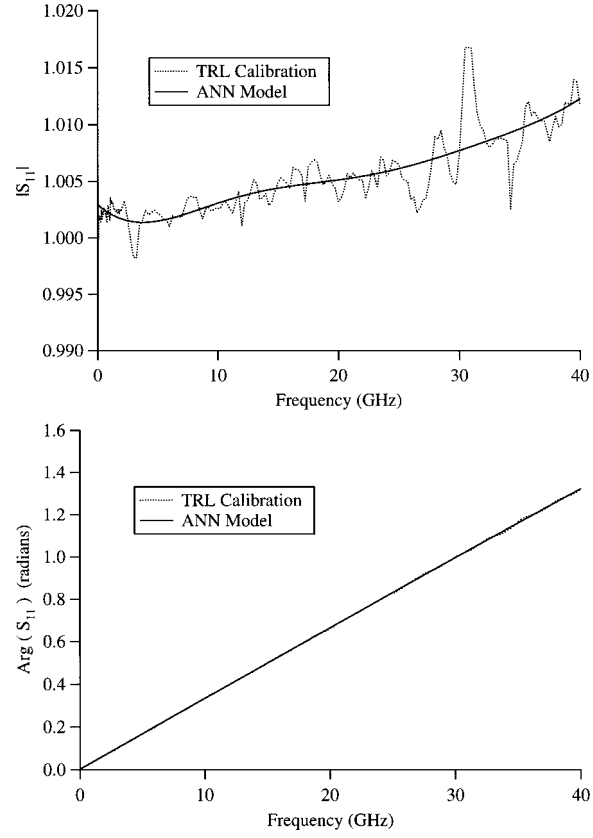

Figure 6. Magnitude and phase of the reflection coefficients [$|S_{11}|$ and Arg(S_{11})] for the open standard measured by multiline TRL and ANN modeling.

trained using the same five points. However, it should be pointed out that using an ANN, trained on only a few points, works for well-behaved standards but could be problematic if the standard contains a resonance.

Next, we developed ANN models for each of the OSLT standards using five hidden neurons and all the 192 measured points, because we already had the data on hand. Figures 6–8 show the magnitude and phase of S_{11} using both measured and ANN model data for the open, short, and load standards, respectively. Figure 9 shows the magnitude and phase of S_{21} using the measured and ANN model data for the thru standard. Notice that the ANN models for each standard follow the trends of the measured data, but avoid the scatter of multiline TRL calibrated measurements. Whether or not this scatter is real, we see that ANNs follow general trends but omit the scatter, which is usually desirable in a model as long as the scatter is less than the repeatability of the measurements. In Figures 6 and 7, the measured magnitudes of the reflection coefficient for the open and short standards are slightly greater than 1, which is not possible for passive devices. This discrepancy can be attributed to random errors in the TRL calibration, which are typically as high as 0.02 at 40 GHz. Our measurements never exceed 1 by more than this repeatability error. A similar argument can be made for the transmission coefficients of the thru standard.

3.2. Calibration Comparisons

We performed two OSLT calibrations, one using the calibrated measurement data of the standards and the other using the ANN models of the standards. We calibrated a 19-mm CPW transmission line; using both the OSLT calibrations, and compared the results to measurements calibrated directly using the benchmark multiline TRL calibration. Figure 10 compares the magnitude and phase of the scattering-parameter

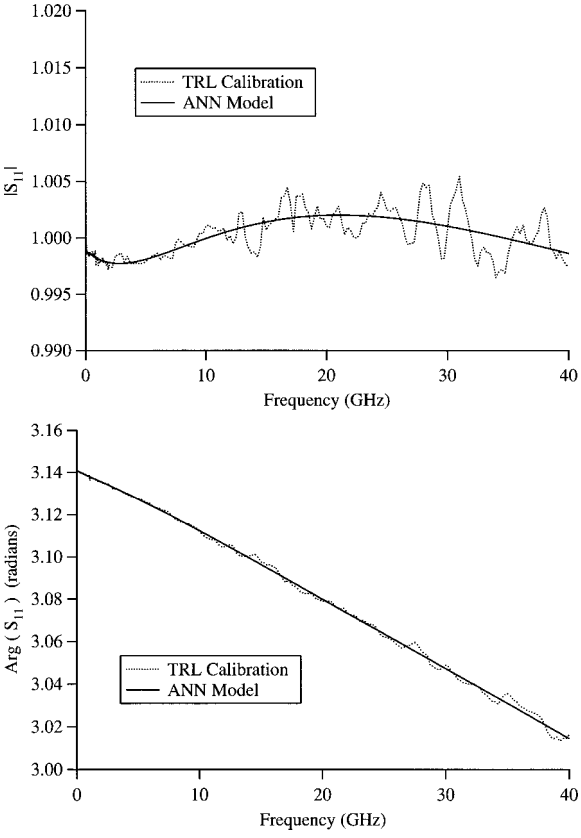

Figure 7. Magnitude and phase of the reflection coefficients [$|S_{11}|$ and Arg(S_{11})] for the short standard measured by multiline TRL and ANN modeling.

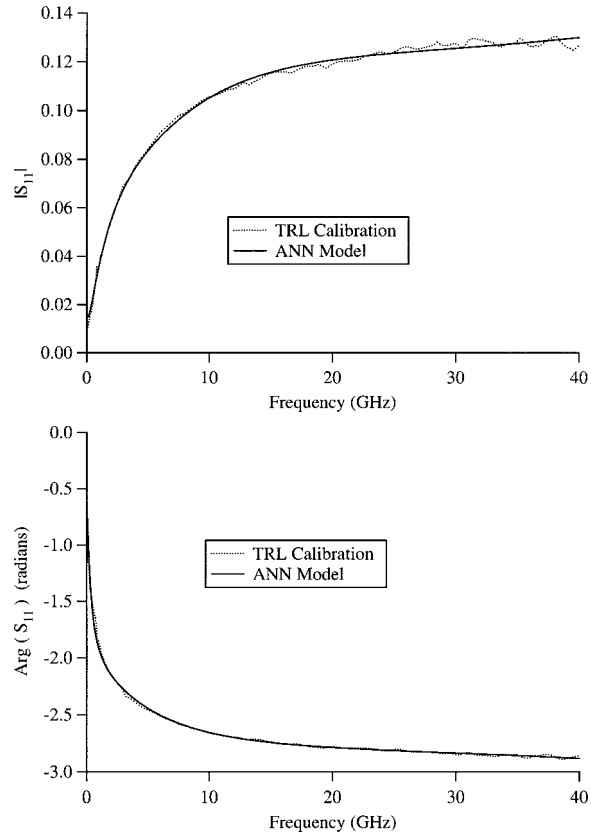

Figure 8. Magnitude and phase of the reflection coefficients [$|S_{11}|$ and Arg(S_{11})] for the load standard measured by multiline TRL and ANN modeling.

data [$|S_{11}|$, Arg(S_{11}), $|S_{21}|$, Arg(S_{21})] for all the three calibrations. The agreement is remarkably good.

To get a more quantitative idea of the differences, we plotted the maximum vector differences of the scattering parameters ($|\Delta S_{ij}|$) for the 19-mm line between the two OSLT calibrations and the multiline TRL calibration. Figure 11 illustrates the differences. Not surprisingly, the OSLT calibration, using the calibrated-measurement data, compares better to the multiline TRL calibration, because they both make use of the same calibration data. However, the OSLT using the ANN models still compares well with less than a 0.02 difference in magnitude at all frequencies. The difference here does not necessarily mean that the OSLT, using ANN models, is in error. The differences could be due to the presence of noise in the TRL calibration that the ANN models avoided. Regardless of the source of error, a 0.02 difference between two on-wafer calibrations spanning 40 GHz is impressive, considering that the repeatability between two multiline TRL calibrations is usually on the order of 0.015.

4. ON-WAFER OSLT WITH VARYING LOADS

The assumption made in the previous section was that the standards can be reproduced from wafer to wafer with little variation. Kirby et al. [23] studied variations in OSLT standards from wafer to wafer on a CPW calibration set designed for GaAs substrates, and found that open, short, and thru standards can be reproduced with minimal variance, but that load standards exhibit a significance difference among the wafers they studied. Furthermore, they discovered that RF variations in the load terminations correlate directly to their measured DC resistances.

Here, we demonstrate that on-wafer OSLT calibrations of VNAs can be further improved by applying ANNs to model the correlation between DC resistance and RF variations in load terminations [13]. The ANNs are trained with

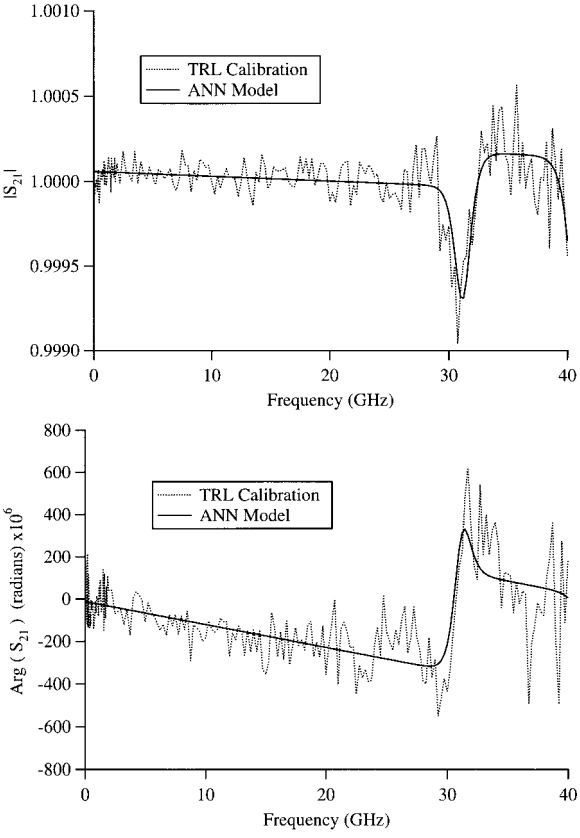

Figure 9. Magnitude and phase of the transmission coefficients [$|S_{21}|$ and Arg(S_{21})] for the thru standard measured by multiline TRL and ANN modeling.

measurement data obtained from a benchmark multiline TRL calibration. The open, short, and thru standards do not vary significantly from wafer to wafer, so we also model these standards using ANNs trained with calibrated measurement data chosen from an arbitrary wafer. We assess the accuracy of five OSLT calibrations with varying load terminations using the ANN-modeled standards, and find that they compare favorably (a difference in magnitude of less than 0.04 at most frequencies) to the benchmark multiline TRL calibration over a frequency range of 66 GHz.

4.1. Modeling the Standards

In this study, the OSLT and multiline TRL standards and devices were constructed of CPW transmission lines fabricated from 4.5 μm plated gold on a 625 μm thick GaAs. The load terminations were composed of TiWN (titanium tungsten nitride) thin film resistive material [23]. The four line standards included a thru line and three additional lines that were 0.9552, 1.239, and 1.764 mm longer. All of the standards were measured using on-wafer probes. For each standard, we measured scattering parameters at 165 frequencies from 1 to 67 GHz. The OSLT standards were characterized using a multiline TRL calibration with the reference plane shifted back to the probe-tips.

Because the open, short, and thru standards did not vary significantly from wafer to wafer, we modeled these standards with ANNs using calibrated measurement data chosen from an arbitrary wafer. The ANN architecture for the open, short, and thru standards consisted of one input (frequency) and two outputs (the real and imaginary components) for each measured scattering parameter. Because we measured reflection coefficients for the two terminations at both the ports and all the four scattering parameters of the thru connection, we ended up with eight ANN models, excluding the load. From our previous study in [12], we determined that five neurons were sufficient for the hidden layer. We trained each model of the standards using all 165 frequencies because we already had the data on hand.

The ANN architecture for the load standards consisted of two inputs (frequency and DC resistance) and two outputs (the real and imaginary components) for the impedance parameters at each port. Owing to a systematic difference between the load measurements at port 1 and port 2, we were unable to generate one model that included both ports, so we settled on separate models for each port. Ten neurons were chosen for the hidden layers because the ANN models for the loads included an additional input compared to the other standards. The measured DC resistances for the loads are listed in Table I. For each port, we trained the models using 3 of the 5 loads. We chose loads 1, 4, and 5 because load 1 had the lowest DC resistance, load 5 had the highest, and load 4 had an intermediate value. It is important to train ANNs at the expected boundary values of the input parameter space to ensure good performance of the model [1]. By purposely not training the ANN with loads 2 and 3, we could test how effectively the model behaved at other DC resistances. Figure 12 shows the real and imaginary components of port 1 impedance, Z_1, of both measured and ANN-modeled data for the 5 load standards. Likewise, Figure 13 shows the real and imaginary components of port 2 impedance, Z_2, of both measured and ANN-modeled data for the 5 load standards. Once again, we see that ANNs follow general trends while omitting the scatter.

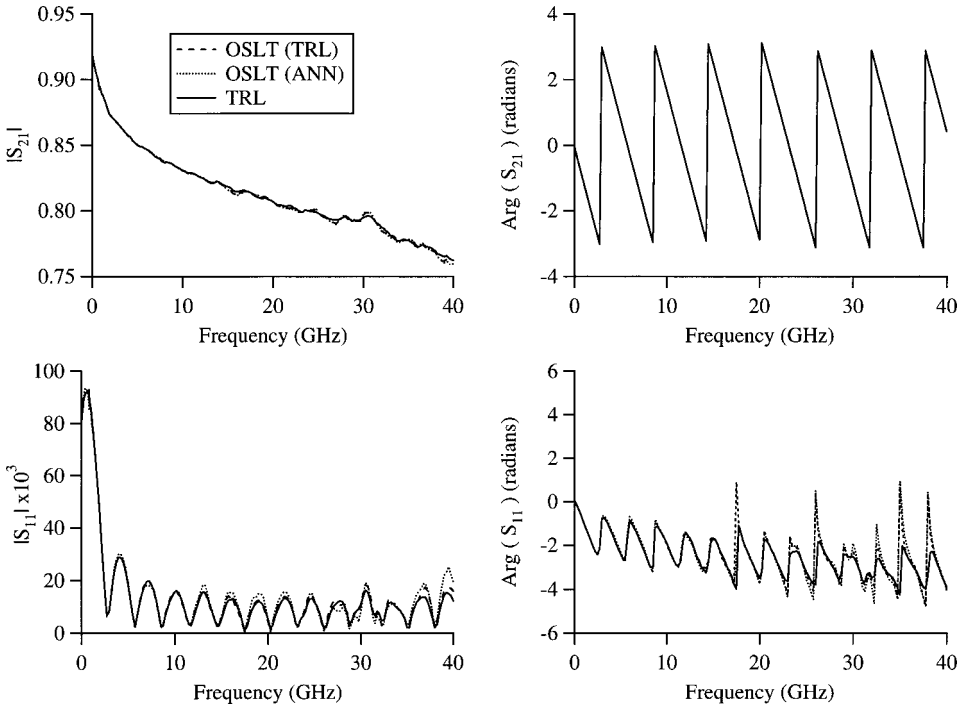

Figure 10. Magnitude and phase of the scattering parameters of a calibrated 19-mm CPW transmission line.

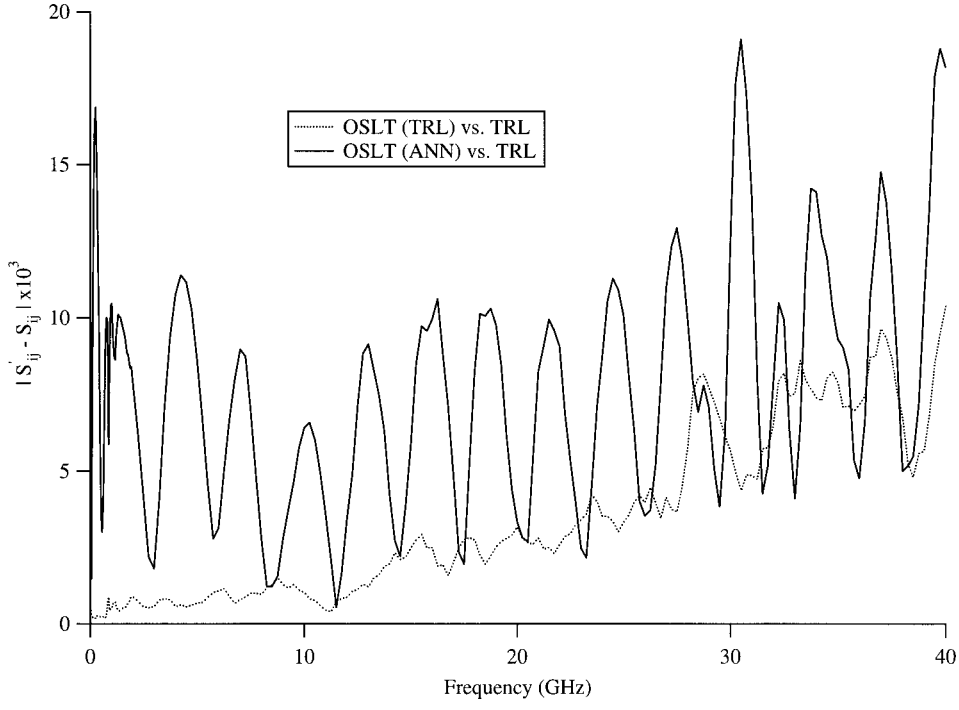

Figure 11. Magnitude of the scattering parameter differences ($|\Delta S_{ij}|$) of a calibrated 19-mm CPW transmission line.

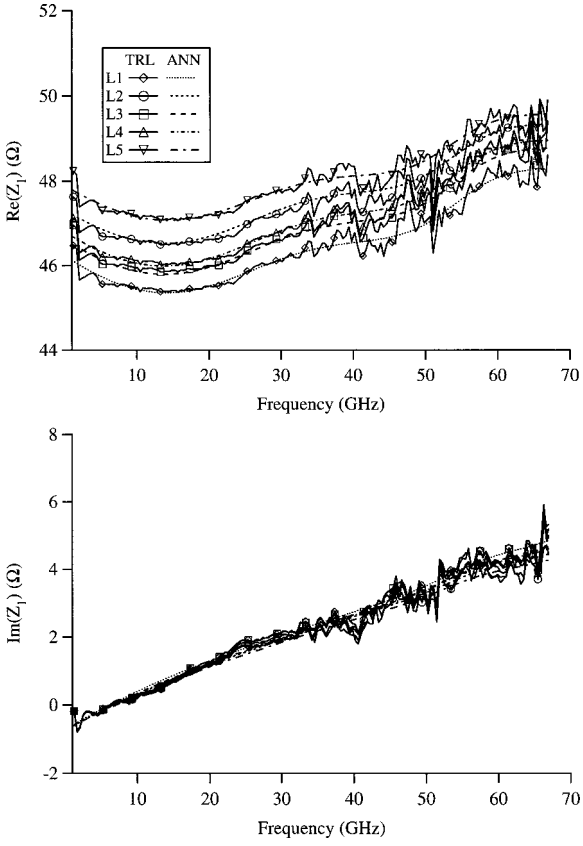

Figure 12. Real and imaginary components of Z_1 for the load standards measured by multiline TRL and modeled by an ANN.

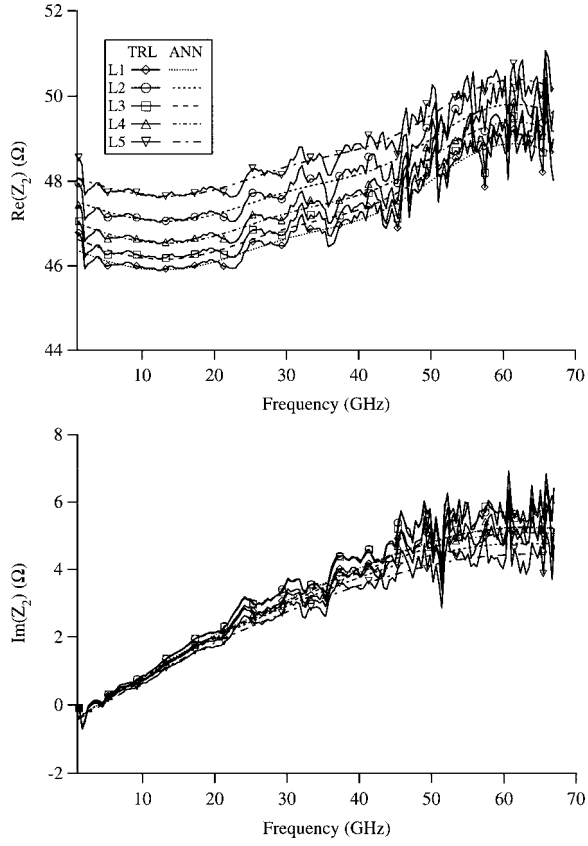

Figure 13. Real and imaginary components of Z_2 for the load standards measured by multiline TRL and modeled by an ANN.

4.2. Advantages of ANN Models

One of the advantages of using ANN models as opposed to calibrated-measurement files is the compact description possible with an ANN. For example, the ANN model we developed for the load at port 1 required 62 real-valued parameters to generate complex S-parameters as a function of frequency and DC resistance. In contrast, a single measurement file contains 495 real-valued numbers (165 frequency points plus the real and imaginary components at each point). If a measurement database of just 5 loads were utilized, then the combined files would contain 2475 real-valued numbers.

We also explored the use of ANN models for extrapolation outside the bounds of the training data. (Generally, it is believed that ANN models are good at interpolating but not extrapolating.) We did this by training an ANN model at port 1 using 3 of the 5 loads once again, but this time we chose loads 2, 3, and 4. By purposely not training the ANN model with loads 1 and 5, we could test how effective the model behaved at extrapolating. Surprisingly, both the interpolating and extrapolating ANN models exhibited almost identical deviations between measured and predicted values. This predicts well for the application of ANN models to our loads, because it is conceivable that other wafers may possess DC resistances slightly outside the range of the 5 loads we used to train the models.

TABLE I. Measured DC Resistances of the Five Load Terminations

	DC Resistance (Ω)	
Load	Port 1	Port 2
1	44.73	45.01
2	45.85	46.13
3	45.20	45.27
4	45.38	45.64
5	46.45	46.71

4.3. Calibration Comparisons

We performed five OSLT calibrations, each one making use of the same ANN-modeled open, short, and thru standards as well as the ANN-modeled loads with their respective DC resistances. We calibrated a 1.764-mm long CPW transmission line using each of the OSLT calibrations and compared the results to measurements calibrated directly using the benchmark multiline TRL calibration. Figure 14 compares the magnitudes of S_{21} and S_{11} for all the six calibrations. The agreement is remarkably good except at a few points where the multiline TRL calibration shows a lot of scattering.

To obtain a more quantitative idea of the differences, we plotted the maximum magnitude of the vector differences of the scattering parameters [$\max(|S_{ij}|)$] for the 1.764-mm line for each of the OSLT calibrations and the multiline TRL calibration. Figure 15 illustrates the differences. All the OSLT calibrations using ANN-modeled standards compare favorably to the benchmark multiline TRL calibration, with a difference of less than 0.04 in magnitude at most of the frequencies over the 66 GHz frequency range. Not surprisingly, the OSLT calibrations for loads 2 and 3 show slightly higher differences because they were not used to train the ANN model. The differences between the 5 OSLT calibrations and the TRL calibration do not necessarily mean that the OSLT calibrations are in error. The differences are likely due to the presence of noise in the TRL calibration that the ANN models avoided. Regardless of the source of error, a 0.04 difference between the two on-wafer calibrations spanning 66 GHz is impressive, considering that the repeatability between the two multiline TRL calibrations is usually on the same order.

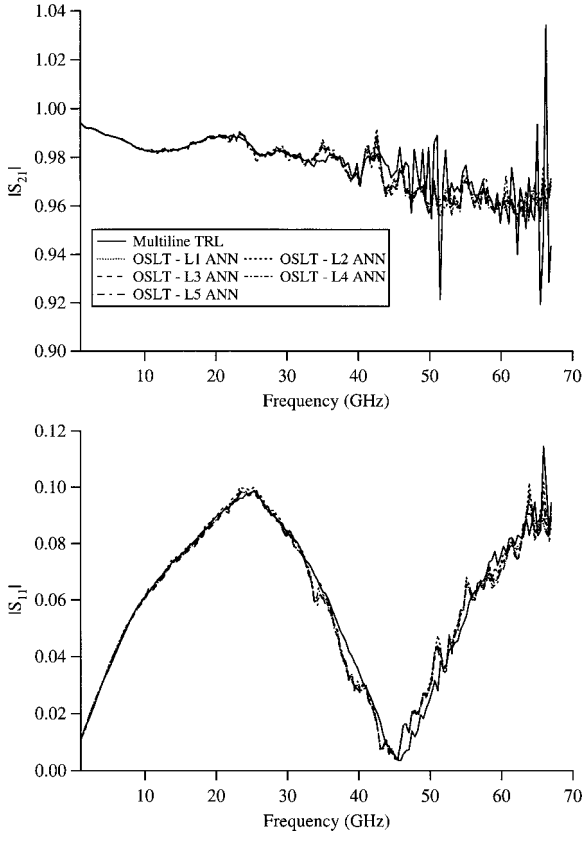

Figure 14. Magnitudes of S_{21} and S_{11} for a calibrated 1.764-mm CPW transmission line.

5. ON-WAFER LRM

Another popular compact calibration method is line-reflect-match (LRM), which requires only a short transmission-line connection, a load, and a reflection [11]. Here, the reference impedance is set to that of the standard load. As shown above, the impedance of many on-wafer loads, however, is nonideal, which can lead to significant errors in LRM calibrations.

Here, we modeled a load using an ANN to improve an on-wafer LRM calibration [15]. The ANN is trained with measurement data obtained from a single-line TRL calibration. Using a single-line TRL calibration enables us to build an effective model of the load using minimal real estate on the wafer. This methodology results in an LRM calibration with less overall error than by simply applying the single-line TRL calibration [24]. The accuracy of the LRM calibration using the ANN-modeled load compares favorably to a benchmark multiline TRL calibration with an average worst-case scattering parameter error bound of 0.017 over a 40-GHz frequency range.

5.1. Modeling the Load

In this study, the LRM and multiline TRL standards and devices were constructed with CPW transmission lines fabricated from 1.5 μm gold conductors on a 500 μm thick semi-insulating GaAs [24]; the gold center conductor 73 μm wide, and separated from the ground plane by 49 μm gaps. The five line standards included a 0.55-mm thru line and four additional lines that were 2.135, 3.2, 6.565, and 19.695 mm longer. All the standards were measured using on-wafer probes. For each standard, we measured scattering parameters at 192 frequencies from 0.5 to 40 GHz.

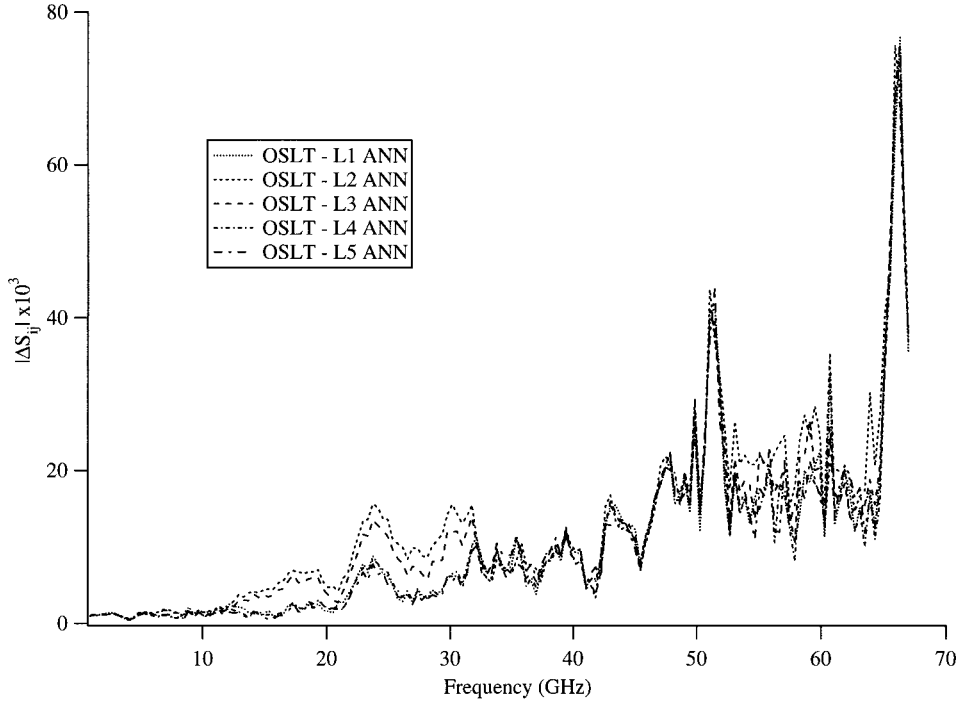

Figure 15. Magnitudes of the scattering parameter differences of a calibrated 1.764-mm CPW transmission line.

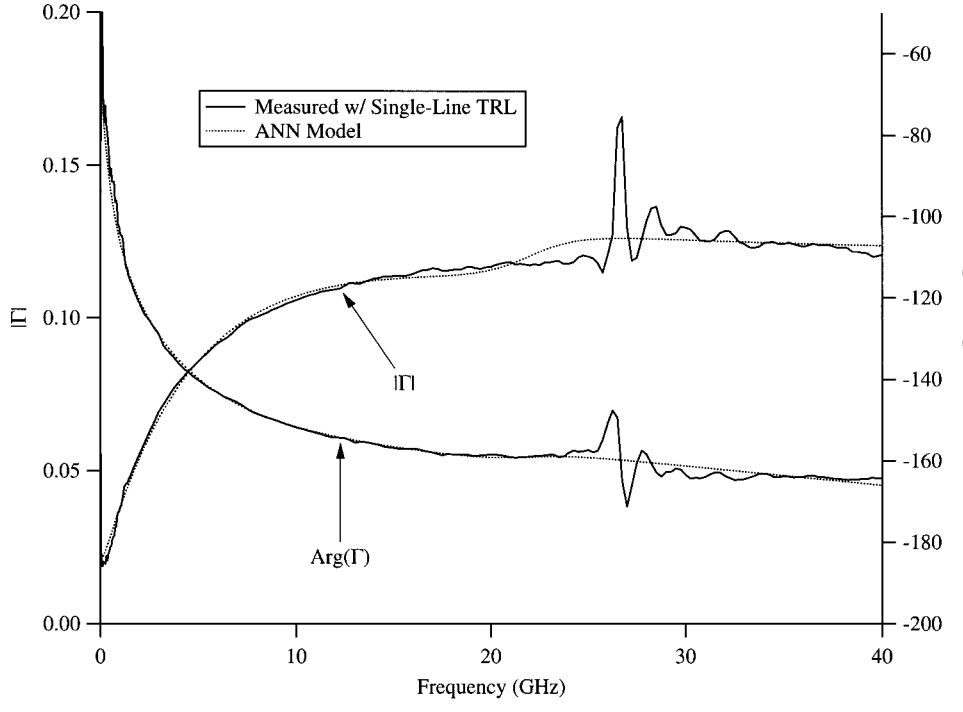

Figure 16. Magnitude and phase of measured and modeled scattering parameters of the on-wafer load for the LRM calibration.

In Figure 16, we plot measurements of magnitude and phase of the load's reflection coefficients. They were determined by a TRL calibration using only the thru connection and the 2.135-mm line, and applying an impedance transformation to the calibration, which yielded the measured *S*-parameters referenced to 50 Ω [25]. The use of only a single line explains the inaccuracy at multiples of 26.65 GHz, where the difference in line lengths corresponds to a multiple of half a wavelength [10]. The figure shows that the load deviates significantly from 50 Ω over the frequency range of 40 GHz.

The ANN for the load standard consisted of one input (frequency) and two outputs (the real and imaginary components) for the S-parameters. From previous experience [12], five neurons were chosen for the hidden layers. Figure 16 shows the magnitude and phase of the reflection coefficients of both measured and ANN model data for the load standard. Notice that the ANN model for the load standards follows the trends of the measured data, but avoids the spike near 26.65 GHz as well as scatter of the TRL calibrated measurements.

5.2. Calibration Comparisons

First, we compare two consecutive multiline TRL calibrations, using all five lines, to assess the limitations on calibration repeatability caused by contact error and instrument drift. The technique of [26] was used to determine an upper bound on this repeatability error. Briefly, the comparison determines the upper bound for $|S'_{ij} - S_{ij}|$ for measurements on any passive device, where S'_{ij} are the scattering parameters of a device measured with respect to the first calibration and S_{ij} are the scattering parameters measured with respect to the second calibration. The bound is obtained from a linearization, which assumes that the two calibrations are similar to the first order. The result, plotted as a solid curve in Figure 17, roughly indicates the minimum deviation between any pair of calibrations. The average of the worst-case error bounds for repeatability was 0.013.

We then compared the single-line TRL calibration, which was used to develop the ANN model, to the multiline TRL calibration. The result is plotted in Figure 17. Because we used only the 2.135-mm line standard, our calibration accuracy is poor near multiples of 26.65 GHz. Otherwise, the single-line TRL calibration is nearly as accurate as the multiline TRL calibration at most frequencies.

We next assessed the accuracy of the LRM calibrations by comparing them to a 50 Ω multiline TRL calibration. First, we compare a simple

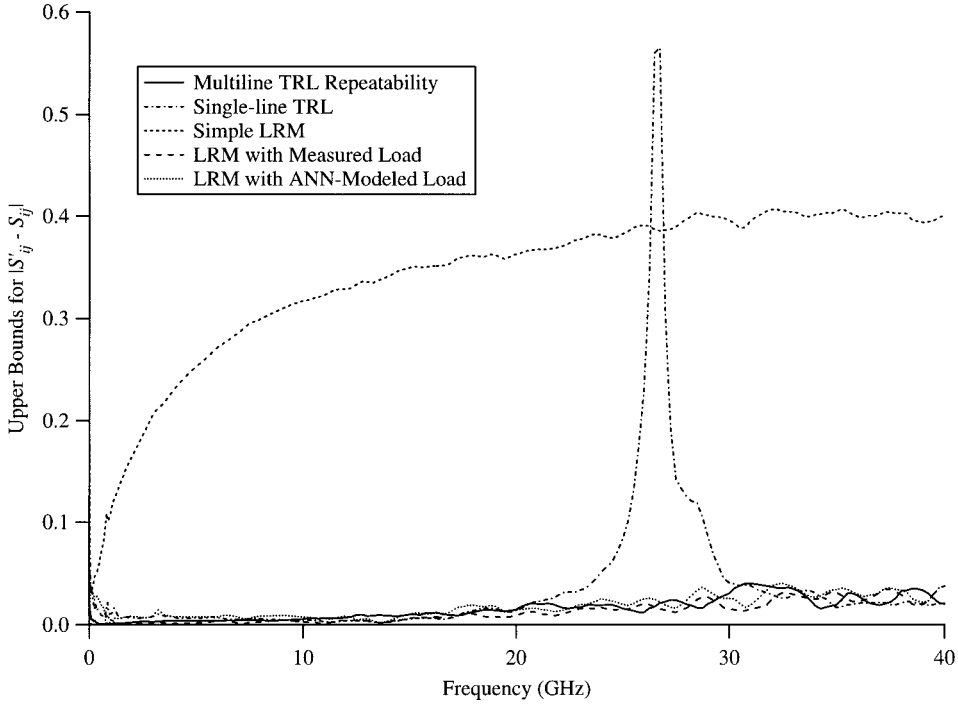

Figure 17. Worst-case error bounds between measurements of passive devices from on-wafer LRM and TRL calibrations and the multiline TRL calibrations.

LRM calibration, where the load is assumed to be ideal, and the multiline TRL calibration. Figure 17 illustrates a large difference because the reference impedance of the LRM calibration, which is equal to the impedance of the nonideal load, deviates significantly from 50 Ω.

To see how accurate the best LRM calibration was, we compared the multiline TRL calibration to the LRM with a fully characterized load, which involved calibrating the load with the benchmark multiline TRL calibration and using the calibrated measurement data file to define the load. This comparison is once again shown in Figure 17. The average of the worst-case error bounds for this calibration was 0.011.

Finally, Figure 17 shows the worst-case error bounds for the LRM calibration based on the ANN-modeled load. Here, the average of the worst-case bounds was 0.017.

6. COAXIAL LRM

We also modeled a coaxial load using an ANN to improve a coaxial LRM calibration, as shown in Figure 18 [14]. Just as in Section 5, where we modeled on-wafer LRM calibrations, we compared a number of calibrations. First, two consecutive multiline TRL calibrations, using all three airlines, were compared to assess the limitations on calibration repeatability. The result, plotted as a solid curve in Figure 19, roughly indicates the minimum deviation between any pair of calibrations. The average of the worst-case error bounds for repeatability was 0.013.

We then compared the single-line TRL calibration to the mutliline TRL calibration. The result is plotted in Figure 19. Other than the poor accuracy near multiples of 6.67 GHz, the single-line TRL calibration is nearly as accurate as the multiline TRL calibration at most frequencies.

We next assessed the accuracy of the LRM calibrations by comparing them to the 50 Ω multiline TRL calibration. Figure 19 shows the maximum possible differences for the simple LRM, the LRM with the fully characterized load, the LRM with a circuit-modeled load, and the LRM with the ANN-modeled load. The average of the worst-case error bounds for the LRM with the fully characterized load was 0.016, the average for the ANN-modeled LRM calibration was 0.024, and the average for the circuit-modeled LRM was 0.034.

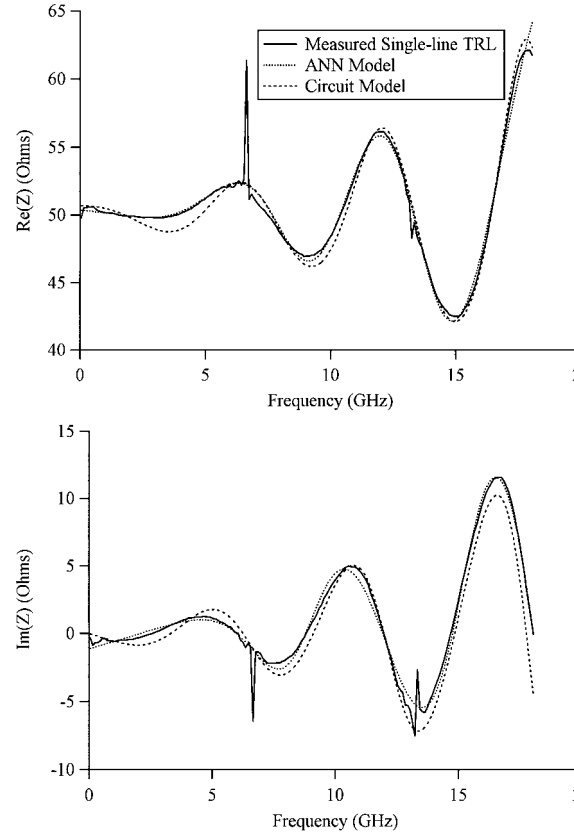

Figure 18. Real and imaginary components of the measured and modeled impedance of the coaxial load for the LRM calibration.

7. OTHER APPLICATIONS

In this section, we summarize other examples of how ANNs have been applied to RF and microwave measurements. In particular, we discuss how two groups of researchers have used ANNs to model the transformation from measured reflection coefficients to permittivity values for liquids. We also examine how scientists have used ANNs to determine the moisture content of wheat from microwave transmission coefficient measurements.

7.1. Permittivity Determination from Open-ended Coaxial Probes

Open-ended coaxial probes are commonly used nondestructive tools for measuring the permittivity of dielectric materials. The coaxial probe, which is connected to a VNA, is pressed against a sample, and the measured reflection coefficient is used to determine the permittivity of the sample. The transformation from reflection coefficient to permittivity requires an accurate model.

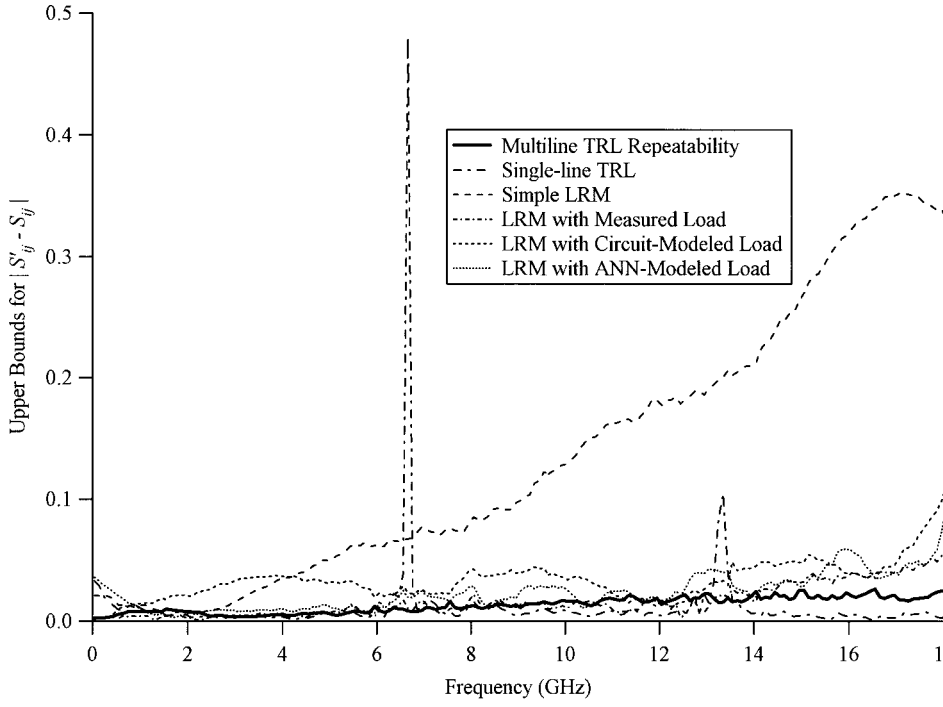

Figure 19. Worst-case error bounds between measurements of passive devices from coaxial LRM and TRL calibrations and the multiline TRL calibrations.

Several approaches have been taken, including equivalent-circuit models, variational techniques, and full-wave analyses [27–29].

Recently, ANNs have been developed as a means of transforming the measured reflection coefficients of liquids, using an open-circuited coaxial probe, to their respective permittivity values. Two groups of researchers have shown that this can be done for different sets of fluids. Figure 20 illustrates the measurement setup.

Tuck and Coad implemented an ANN using training data from nine different liquids in the frequency range of 200 MHz to 16 GHz [30]. In another study, Bartley et al. [31] implemented an ANN using training data from eleven liquids (different mixtures of water and isopropyl alcohol) in the frequency range of 200 MHz to 6 GHz. Both of these studies suggest that ANNs can be successfully applied to determine the dielectric properties of materials from uncalibrated reflection coefficient measurements made on an open-ended coaxial probe.

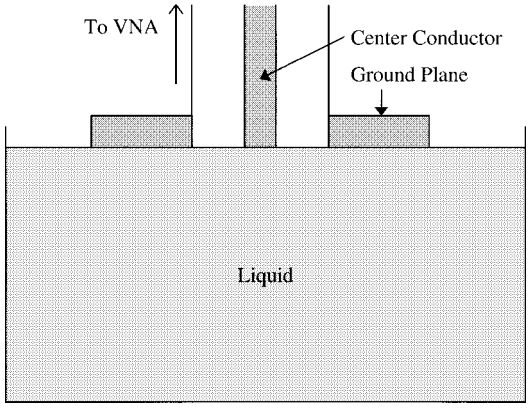

Figure 20. Using an open-ended coaxial probe for measuring reflection coefficients of liquids.

7.2. Determining Moisture Content of Wheat from Transmission Measurements

Bartley et al. [32] also applied an ANN to determine the moisture content in wheat from microwave transmission measurements. The ANN was trained for moisture contents between 10.6% and 19.2% , which is referred to as "wet basis," and bulk densities varying from 0.72 to 0.88 g/cm^3. Measurements were made from free-space transmission-coefficient measurements on layers of wheat placed between two antennas connected to a VNA at eight frequencies ranging from 10 to 18 GHz. Figure 21 illustrates the measurement setup.

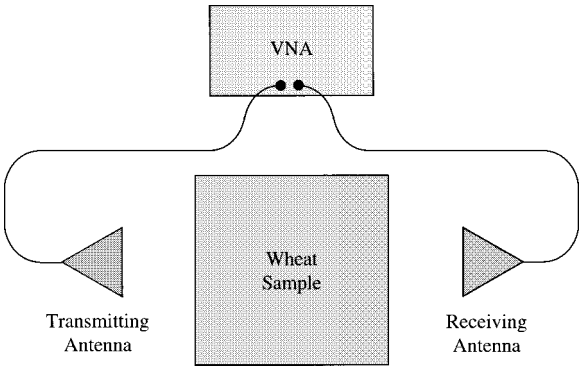

Figure 21. Measuring the free-space transmission coefficient of a wheat sample placed between two horn antennas.

The ANN architecture consisted of one hidden layer with fifteen neurons. Sixteen inputs (the magnitudes and phases of each of the eight measured transmission coefficients) were used for the ANN model. The one output was moisture content. For the 179 sample measurements, Bartley *et al.* calculated the mean squared error between the ANN model and the measured results to be 0.028. Here, the authors point out that this method has the potential for on-line, nondestructive moisture content measurement for flowing grain.

8. POTENTIAL APPLICATIONS

In this section, we discuss some potential applications of ANN models related to RF and microwave power measurements and material characterization. Specifically, we show how ANN models may be used to determine the complex permittivity of low-loss dielectric materials from measured shifts in resonant frequency and quality factor using a split-post resonator. We also illustrate how lengthy measurement times for microcalorimetric measurements can possibly be reduced without noticeably degrading accuracy.

8.1. Determining Complex Permittivity Using a Split-Post Resonator

The most accurate way of measuring the complex permittivity of a low-loss dielectric material is by using one of a number of resonator methods [33]. Although usually limited to a single frequency, resonators provide the required accuracy that broadband methods lack. However, the disadvantage of most resonator techniques is the need for accurately machined samples of the material of interest.

Recently, Krupka et al. [34] introduced a new type of resonator that allows for nondestructive permittivity measurements, referred to as the split-post resonator, shown in Figure 22. Briefly, the permittivity of a sample is determined from shifts in the quality factor and resonant frequency from measurements taken with and without the sample in place. Krupka et al. utilize the Rayleigh–Ritz method to theoretically determine the shift in resonant frequency and quality factor from the complex permittivity and sample thickness. Using a wide range of permittivities and sample thicknesses, they created a look-up table that is used to calculate the sample permittivity from measured shifts in resonant frequency and quality factor for a given sample thickness. For values that are not explicitly listed in the table, they interpolate between the two closest values.

Researchers at the National Institute of Standards and Technology (NIST) are currently developing an independent mode-matching model for the split-post resonator to compare with the method of Krupka et al. In a similar manner as described above, they will develop a model to determine the shift in resonant frequency and quality factor from the complex permittivity and sample thickness. But rather than creating a look-up table, they are interested in developing an ANN model, trained by data from the mode-matching technique, to provide the complex permittivity for a given sample thickness from measured shifts in resonant frequency and quality factor. The ANN will provide an efficient model for the transformation that would otherwise be time-consuming using the mode-matching computations each time.

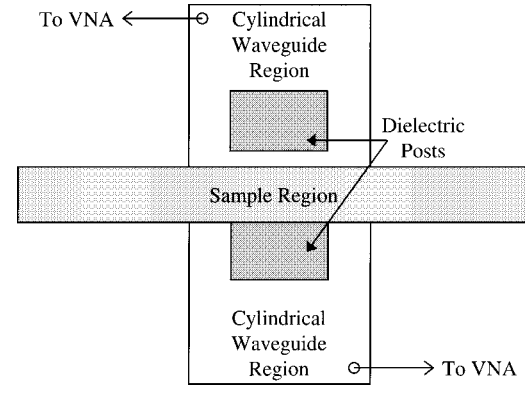

Figure 22. Cross-sectional diagram of a split-post resonator.

8.2. Microcalorimetric Power Measurements

The measurement of microwave power is a fundamental test requirement necessary for determining output levels of signal generators, transmitters, and radar, just to name a few. Invariably, commercial power sensors are ultimately traceable to measurements made by primary national standards laboratories, most of which utilize a water-bath microcalorimeter and a reference standard for coaxial and waveguide measurements. The reference standards are usually substitution-type bolometric power detectors, which use heat sensitive resistors terminating a transmission line that absorbs microwave power [35].

However, not all the microwave energy incident on a power detector is absorbed by the bolometer element. Some of the power is dissipated in the connector, the transmission line, and the bolometer mounting structure, and some additional power is lost to leakage in the mount. These factors result in a dimensionless measurement error called the mount efficiency, which is always less than one. Additionally, the bolometer elements are not heated identically by the same amounts of RF and DC power, which is referred to as the RF-DC substitution error. The combination of these two errors is defined as the effective efficiency, which is independent of mismatch corrections.

Customers who wish their devices to be directly traceable to a national standards laboratory submit their devices for calibration. After the measurements are complete, the customer receives a table of effective efficiencies for the frequencies measured. Because a typical measurement of 360 frequency points requires approximately 48 hours due to the time required for the thermopile to stabilize at each point, ANNs have the potential to lessen measurement times by reducing the number of frequency points. An ANN model, could in principle, be trained to interpolate the effective efficiency between a reduced set of measurements, especially for devices that have been previously measured and are known to behave correctly, without unpredictably large spikes that occur over a short frequency span.

Figure 23 shows a typical measurement of effective efficiency for a coaxial bolometer mount versus frequency. Here, 360 points were measured at frequencies ranging from 0.05 to 18 GHz. The effective efficiency decreases monotonically for frequencies above 3 GHz. If we were to take a conservative approach, then we could train an ANN to interpolate the values of effective efficiency between 5 and 18 GHz. Figure 23 shows open circles that represent a reduced set of 27 measurements between 5 and 18 GHz. With this subset of measurements, we trained an ANN and tested it with all of the original measurement points made between 5 and 18 GHz. The results predicted by the ANN are shown as small dots in Figure 23. Figure 24 shows the differences between the measurements of effective efficiency and the values predicted by the ANN model for this subset of frequencies. Also plotted in Figure 24 is the reported uncertainty of the measurements. It can clearly be seen that the errors made by the ANN model fall far below the reported uncertainties. Even by using this conservative approach, we could reduce the calibration time to one third of its usual duration, thereby potentially saving money to the customer and increasing the throughput.

In addition to reducing measurement times for microcalorimeter measurements without noticeably degrading accuracy, ANNs can potentially be used in other areas where measurement times are lengthy, such as the determination of noise parameters.

8.3. Comparing Nonlinear Vector Network Analyzers

A class of instruments known as nonlinear vector network analyzers (NVNAs) [36–39] characterize nonlinear devices by supplying large-signal RF stimuli and measuring the resulting signals at the boundaries of the device under test. Unlike devices operating in the linear region, nonlinear devices cannot be adequately characterized by scattering parameters because nonlinearities transfer energy from the stimulus frequency (or frequencies) to products at new frequencies. NVNAs measure incident and reflected wave variables at stimulus frequencies and their harmonics (and intermodulation products). As the exact spectrum of stimuli varies from one instrument to another, measurements made on different NVNAs cannot be directly compared.

Researchers at NIST are currently developing a set of nonlinear verification devices and a method to compare NVNA systems [40]. As mentioned earlier, because no two systems have identical stimuli, connections, and port impedances, measured parameters cannot be directly compared. To overcome this problem, Remley et al. [40] have

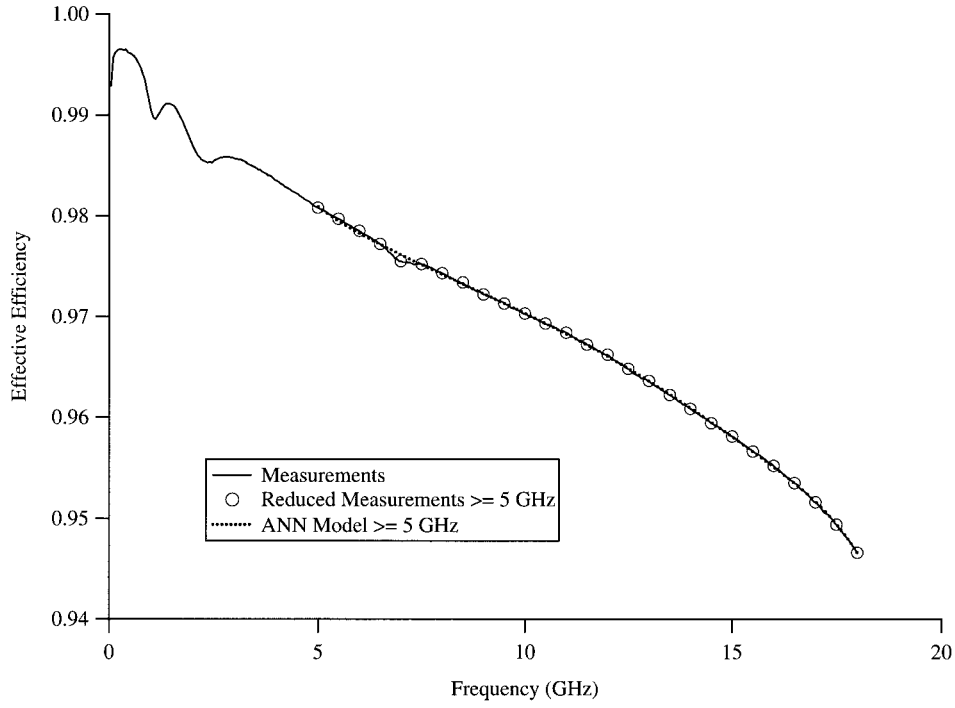

Figure 23. A typical measurement of effective efficiency for a coaxial bolometer mount versus frequency.

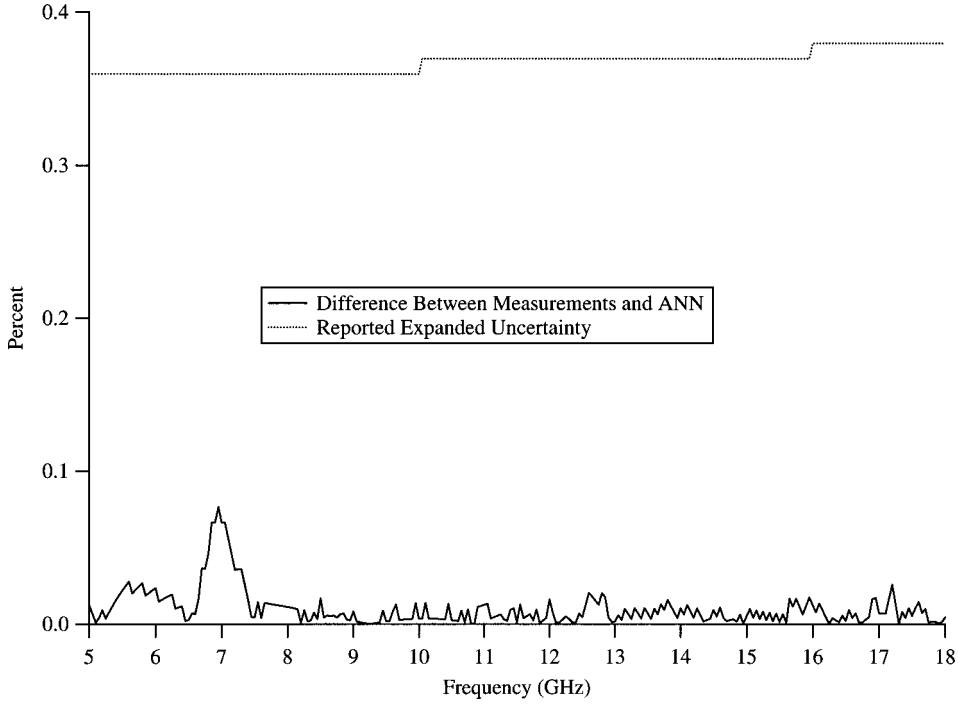

Figure 24. Differences between measurements of effective efficiency and values predicted by the ANN model.

introduced a method where predictive comparisons are first carried out for a system between the measured output and the output from a model of a given verification device for the same excitation conditions. Then the predictive comparisons for each system are compared, holding the verification device model invariant. The difference between predictive comparisons gives parameters for checking measurement consistency between NVNAs.

ANNs have the potential to improve this comparison. If an ANN model were trained using data from a verification device measured on a reference system for a number of stimuli and port impedances, then it would be possible to simply compare the output from another system with the output predicted by the ANN model applying the same excitation conditions. The possible use of ANN models for such an application is currently being investigated.

9. CONCLUDING REMARKS

We have successfully applied ANNs to model on-wafer and coaxial lumped-element calibration standards, and have shown that calibrations that make use of ANN-modeled standards compare favorably to benchmark multiline TRL calibrations. In modeling the standards, we quantified the training errors and training times as a function of both the number of training points and the number of neurons in the hidden layer.

In practice, ANN-modeled calibration standards can be easily implemented using existing or custom software packages. In our case, we utilized MultiCal [10], a free program developed by the National Institute of Standards and Technology, to perform our multiline TRL and LRM calibrations. The internal software on any commercial network analyzer can also be used if the user has confidence in another calibration method. Then, once the lumped-element standards are measured, one of a number of ANN programs may be used to model the standards. We used software developed by Zhang et al. [16] to construct our ANN models. For the OSLT experiments, we wrote custom software to perform the calibrations with exported ANN models, using the equations found in refs. 11 and 21.

We have shown that ANN models offer a number of advantages over using calibrated measurement data files or equivalent circuit models, namely:

(1) They do not require detailed physical models.
(2) Calibration times can be reduced because only a few training points are required to accurately model the standards.
(3) ANN model descriptions are much more compact than large measurement data files.
(4) ANN models, trained on only a few measurement points, can be much more accurate than direct calibrations, when limited calibration data are available.
(5) They are less susceptible to the noise inherent in measured data.
(6) ANN models are able to accurately model loads with measured DC resistances slightly outside their training range.

We have also summarized other current applications of ANNs to RF and microwave measurements. In particular, we discussed how two groups of researchers used ANNs to model the transformation from measured reflection coefficients to permittivity values for liquids, and we examined how scientists used ANNs to determine moisture content of wheat from microwave transmission coefficient measurements.

We have also discussed some potential applications of ANN models related to RF and microwave power measurements and material characterization. Specifically, we examined how ANN models may be used to determine the complex permittivity of low-loss dielectric materials from measured shifts in resonant frequency and quality factor using a split-post resonator. We also illustrated how lengthy measurement times for microcalorimeter measurements could possibly be reduced without noticeably degrading accuracy. Finally, we explored the possibility of using ANN models to compare nonlinear vector network analyzers, where comparing measured parameters directly is not practical.

ACKNOWLEDGMENTS

The authors thank Professor Qi-jun Zhang for his help with the NeuroModeler software, Pete Kirby and Lawrence Dunleavy for providing us with the data used in Section 4, Paul Voris for providing us with the data used in Section 8, and Michael Janezic for his discussions regarding materials measurements.

REFERENCES

1. Q.J. Zhang and K.C. Gupta, Neural networks for RF and microwave design, Artech House, Boston, London, 2000.
2. P.M. Watson and K.C. Gupta, EM-ANN models for microstrip vias and interconnects in dataset circuits, IEEE Trans Microwave Theory Tech 44 (1996), 2495–2503.
3. A. Veluswami, M.S. Nakhla, and Q.J. Zhang, The application of neural networks to EM-based simulation and optimization of interconnects in high-speed VLSI circuits, IEEE Trans Microwave Theory Tech 45 (1997), 712–723.
4. G.L. Creech, B.J. Paul, C.D. Lesniak, T.J. Jenkins, and M.C. Calcatera, Artificial neural networks for fast and accurate EM-CAD of microwave circuits, IEEE Trans Microwave Theory Tech 45 (1997), 794–802.
5. F. Wang and Q.J. Zhang, Knowledge-based neural models for microwave design, IEEE Trans Microwave Theory Tech 45 (1997), 2333–2343.
6. P.M. Watson and K.C. Gupta, Design and optimization of CPW circuits using EM-ANN models for CPW components, IEEE Trans Microwave Theory Tech 45 (1997), 2515–2523.
7. A. Patnaik, R.K. Mishra, G.K. Patra, and S.K. Dash, An artificial neural network model for effective dielectric constant of microstrip line, IEEE Trans Antennas Propagation 45 (1997), 1697.
8. M. Vai, S. Wu, B. Li, and S. Prasad, Creating neural network based microwave circuit models for analysis and synthesis, Proc Asia Pacific Microwave Conf, Hong Kong, Dec. 1997, pp. 853–856.
9. G.F. Engen and C.A. Hoer, Thru-reflect-line: an improved technique for calibrating the dual six-port automatic network analyzer, IEEE Trans Microwave Theory Tech 27 (1979), 987–993.
10. R.B. Marks, A multiline method of network analyzer calibration, IEEE Trans Microwave Theory Tech 39 (1991), 1205–1215.
11. D.K. Rytting, Network analyzer error models and calibration methods, Proc 52nd ARFTG Conference, Short Course on Computer-Aided RF and Microwave Testing and Design, Dec. 1998.
12. J.A. Jargon, K.C. Gupta, and D.C. DeGroot, Artificial neural network modeling for improved on-wafer OSLT calibration standards, Int J RF and Microwave CAE 10 (2000), 319–328.
13. J.A. Jargon, P. Kirby, K.C. Gupta, L. Dunleavy, and T. Weller, Modeling load variations with artificial neural networks to improve on-wafer OSLT calibrations, Proc 56th ARFTG Conference Digest, Nov. 2000, pp. 76-88.
14. J.A. Jargon and K.C. Gupta, Artificial neural network modeling for improved coaxial line-reflect-match calibrations, Int J RF and Microwave CAE 11 (2001), 33–37.
15. J.A. Jargon and K.C. Gupta, Artificial neural network modeling for improved on-wafer line-reflect-match calibrations, Proc 31st European Microwave Conference, Sep. 2001, submitted.
16. Q.J. Zhang and his neural network research team, NeuroModeler, ver. 1.2, Department of Electronics, Carleton University, Ottawa, Canada, 1999.
17. Hewlett-Packard, Network analysis: specifying calibration standards for the HP 8510 network analyzer, Product Note 8510-5A, 1997.
18. Hewlett-Packard, Operating and programming manual: HP 8510B network analyzer, Hewlett-Packard, Manual 1987.
19. Wiltron, Model 360B vector network analyzer operation manual, Wiltron Company, Manual 1991.
20. R.B. Marks and D.F. Williams, Verification of commercial probe-tip calibrations, Proc 42nd ARFTG Conference Digest, San Jose, CA, Dec. 1993, pp. 37–44.
21. D.C. DeGroot, K.L. Reed, and J.A. Jargon, Equivalent circuit models for coaxial OSLT standards, Proc 54th ARFTG Conference Digest, Atlanta, GA, Dec. 1999, 103-115.
22. D.F. Williams, R.B. Marks, K. Phillips, and T. Miers, Progress toward MMIC on-wafer standards, Proc 36th ARFTG Conference Digest, Nov. 1990, pp. 73–83.
23. P. Kirby, L. Dunleavy, and T. Weller, The effect of load variations on on-wafer lumped element based calibrations, Proc 54th ARFTG Conference Digest, Nov. 1999, 81–90.
24. D.F. Williams and R.B. Marks, LRM probe-tip calibrations with imperfect resistors and lossy lines, Proc 42nd ARFTG Conference Digest, Dec. 1993, pp. 32–36.
25. R.B. Marks and D.F. Williams, Characteristic impedance determination using propagation constant measurement, IEEE Microwave Guided Lett 1 (1991), 141–143.
26. D.F. Williams and R.B. Marks, Comparison of on-wafer calibrations, Proc 38th ARFTG Conference Digest, Dec. 1991, pp. 68–81.
27. J. Baker-Jarvis, M.D. Janezic, P.D. Domich, and R.G. Geyer, Analysis of an open-ended coaxial probe with lift-off for nondestructive testing, IEEE Trans Instrum Meas 43 (1994), 711–718.
28. D. Misra, On the measurement of the complex permittivity of materials by an open-ended coaxial probe, IEEE Microwave Guided Lett 5 (1995) 161–163.
29. D.V. Blackham and R.D. Pollard, An improved technique for permittivity measurements using a coaxial probe, IEEE Trans Instrum Meas 46 (1997), 1093–1099.
30. D. Tuck and S. Coad, Neurocomputed model of open-circuited coaxial probes, IEEE Microwave Guided Lett 5 (1995) 105–107.

31. P.G. Bartley, R.W. McClendon, and S.O. Nelson, Permittivity determination by using an artificial neural network, IEEE Instrum and Meas Tech Conference 1999, pp. 27–30.
32. P.G. Bartley, S.O. Nelson, R.W. McClendon, and S. Trabelsi, Determining moisture content of wheat with an artificial neural network from microwave transmission measurements, IEEE Trans Instrum Meas 47 (1998), 123–126.
33. J. Baker-Jarvis, R.G. Geyer, J.H. Grosvenor, M.D. Janezic, C.A. Jones, B. Riddle, C.M. Weil, and J. Krupka, Dielectric characterization of low-loss materials: a comparison of techniques, IEEE Trans Dielect Elect Insulation 5 (1998), 571–577.
34. J. Krupka, R.G. Geyer, J. Baker-Jarvis, and J. Ceremuga, Measurements of the complex permittivity of microwave circuit board substrates using split dielectric resonator and reentrant cavity techniques, Seventh International Conference on Dielectric Materials Measurements and Applications, 1996, pp. 21–24.
35. F.R. Clague, A calibration service for coaxial reference standards for microwave power, National Institute of Standards and Technology Technical Note 1374, 1995.
36. M. Sipilä, K. Lethinen, and V. Porra, High-frequency periodic time-domain waveform measurement system, IEEE Trans Microwave Theory Tech 36 (1988), 1397–1405.
37. G. Kompa and F. van Raay, Error-corrected large-signal waveform measurement system combining network analyzer and sampling oscilloscope capabilities, IEEE Trans Microwave Theory Tech 38 (1990), 358–365.
38. M. Demmler, P.J. Taskar, and M. Schlechtweg, On-wafer large signal power, S-parameter and waveform measurement system, Proc. 3rd Int Workshop on Integrated Nonlinear Microwave and Millimeterwave Circuits, 1994, pp. 153–158.
39. J. Verspecht, P. Debie, A. Barel, and L. Martens, Accurate on-wafer measurement of phase and magnitude of the spectral components of incident and scattered voltage waves at the signal ports of a nonlinear microwave device, IEEE MTT-S Int Microwave Symp Dig, 1995, pp. 1029–1032.
40. K.A. Remley, D.C. DeGroot, J.A. Jargon, and K.C. Gupta, A method to compare vector nonlinear network analyzers, IEEE MTT-S Int Microwave Symp Dig, 2001, pp. 1667–1670.

BIOGRAPHIES

Jeffrey A. Jargon received the B.S. and M.S. degrees in electrical engineering from the University of Colorado at Boulder in 1990 and 1996, respectively. He has been with the Radio Frequency Technology Division, National Institute of Standards and Technology (NIST), Boulder, CO, since 1990. His current research interests include calibration techniques for vector network analyzers and artificial neural network modeling of passive and active devices. Jeffrey has authored or co-authored over thirty technical publications and conference presentations, receiving two best paper awards. He is a member of Tau Beta Pi and Etta Kappa Nu, a Senior Member of IEEE, and is a registered Professional Engineer in the State of Colorado. Jeffrey is currently pursuing the Ph.D. degree in electrical engineering at the University of Colorado at Boulder.

K. C. Gupta has been a Professor at the University of Colorado since 1983. Presently, he is also the Associate Director for the NSF I/UCR Center for Advanced Manufacturing and Packaging of Microwave, Optical and Digital Electronics (CAMPmode) at the University of Colorado, and a Guest Researcher with RF Technology Group of National Institute of Standards and Technology (NIST) at Boulder. Dr. Gupta received his B.E. and M.E. degrees in Electrical Communication Engineering from the Indian Institute of Science, Bangalore, India, in 1961 and 1962, respectively, and the Ph.D. degree from the Birla Institute of Technology and Science, Pilani, India, in 1969. Dr. Gupta's current research interests are in the area of computer-aided design techniques (including ANN applications) for microwave and millimeter-wave integrated circuits, nonlinear characterization and modeling, RF MEMS, and reconfigurable antennas. He is the author or coauthor of eight books including Microstrip Line and Slotlines (Artech House, 1979; revised second edition, 1996); CAD of Microwave Circuits (Artech House, 1981; Chinese Scientific Press, 1986; Radio I Syvaz, 1987); Microstrip Antenna Design (Artech House, 1988); and Neural Networks for RF and Microwave Design (Artech House 2000). He has also contributed chapters to the Handbook of Microstrip Antennas (Peter Peregrinus, 1989); the Handbook of Microwave and Optical Components, vol. 1 (John Wiley, 1989); Microwave Solid State Circuit Design (John Wiley, 1988); Numerical Techniques for Microwave and Millimeter Wave Passive Structures (John Wiley, 1989), and Encyclopedia of Electrical and Electronics Engineering (John Wiley 1999). Dr. Gupta has published about 200 research papers and holds four patents in the microwave area. Dr. Gupta is a Fellow of the IEEE (Institute of Electrical and Electronics Engineers, USA); a Fellow of the Institution of Electronics and Telecommunication Engineers (India); a Member of URSI (Commission D, USA); and a Member of the Electromagnetics Academy (MIT, USA). He is a recipient of IEEE-MTTS Distinguished Educator Award, IEEE Third Millennium Medal, a member of the ADCOM for

the MTT Society of IEEE, chair of the IEEE MTT-S standing committee on Education, past co-chair of the IEEE MTT-S Technical Committee on CAD (MTT-1), a member of the IEEE Technical Committee on Microwave Field Theory (MTT-15), a member of IEEE-EAB Committee on Continuing Education, a member of IEEE-EAB Societies Education Committee, and on the Technical Program Committees for MTT-S International Symposia. He is the founding editor of the International Journal of RF and Microwave Computer-Aided Engineering, published by John Wiley since 1991. He is an Associate Editor for IEEE Microwave Magazine, on the editorial boards of IEEE Transactions on Microwave Theory and Techniques, Microwave and Optical Technology Letters (John Wiley), and International Journal of Numerical Modeling (John Wiley, U.K.). He is listed in Who's Who in America, Who's Who in the World, Who's Who in Engineering, and Who's Who in American Education.

Donald C. DeGroot received the Bachelors degree in Electronics Engineering from Andrews University in 1985, and the M.S. and Ph.D. degrees in Electrical Engineering from Northwestern University in 1990 and 1993, respectively. Currently, Don is the Project Leader with the NIST Nonlinear Device Characterization Project. His present research activities include development of large-signal broadband measurement and calibration techniques for the development and validation of nonlinear circuits. Concurrently, Don is Professor Adjoint of Electrical and Computer Engineering at the University of Colorado at Boulder. Prior to joining the RF Electronics Group, Don researched and developed microwave superconducting devices and thin film measurements as a National Research Council Postdoctoral Associate at NIST; studied the high-frequency properties of novel electronic materials at Northwestern University; and designed high-speed instrumentation at Fermi National Accelerator Laboratory. Don has authored or co-authored numerous technical publications and conference presentations, receiving ARFTG Best Paper and Best Poster Paper awards and an URSI Young Investigator Award. Don is a Senior Member of the IEEE, participating in professional conference and events committees.